JACS Au
AN OPEN ACCESS JOURNAL OF THE AMERICAN CHEMICAL SOCIETY

pubs.acs.org/jacsau
Article

Insights into Mechanochemical Solid-State Ball-Milling Reaction: Monitoring Transition from Heterogeneous to Homogeneous Conditions

Eun Sul Go, Eun Ji Hong, Ji Yeong Lee, Tomislav Stolar, Gregory I. Peterson, Franziska L. Emmerling, Kyoungsoo Kim,* and Jeung Gon Kim*

Cite This: JACS Au 2025, 5, 2720−2727

ABSTRACT: As mechanochemical synthesis has advanced significantly, there has been intense interest in understanding the underlying mechanisms of these reactions. Given that many mechanochemical processes are conducted in the solid-state without solvation yet sometimes yield faster reactions than those in solution, we sought to address the following question: Are mechanochemical reactions homo- or heterogeneous? To investigate, we employed a model system involving the mixing and copolymerization of L-lactide (LLA) and D-lactide (DLA), monitored through powder X-ray diffraction (PXRD), nuclear magnetic resonance, and differential scanning calorimetry. *In situ* and *ex situ* PXRD analyses of the mixture of LLA and DLA showed that vibratory ball milling rapidly transformed the initially heterogeneous lactide mixture into a homogeneous phase within one min due to collisions between the balls and the jar. By varying the milling conditions, we were able to regulate the level of mixing, which subsequently influenced the copolymerization outcomes. In the solid-state ball-milling copolymerization of LLA and DLA in the presence of a catalyst and initiator, multiblock copolymers of poly(L-lactic acid) and poly(D-lactic acid) were formed within one min during the early stage of the reaction, when incomplete mixing of the monomers led to a process governed by phase heterogeneity. In contrast, prolonged polymerization promoted conditions approaching homogeneity, ultimately yielding atactic poly(lactic acid). This transition from heterogeneous to homogeneous reactions is a distinctive feature compared to conventional homogeneous reactions, potentially leading to mechano-exclusive reaction designs.

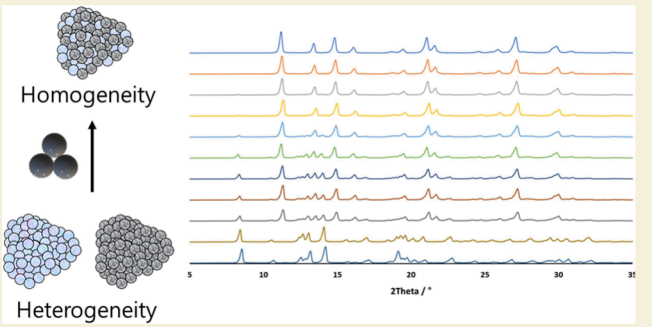

KEYWORDS: *mechanochemistry, ball-milling, homogeneous reaction, heterogeneous reaction*

INTRODUCTION

Mechanochemistry is an eminent chemical synthetic system of great interest.[1−5] Mechanical motion can directly drive chemical transformations, offering distinct advantages over conventional solution-based methods. From a green chemistry perspective, direct mixing and energy delivery of neat or highly concentrated reagents significantly reduce the amounts of solvents.[6,7] The absence of solvent eliminates dilution effects, and the resulting high reactant concentration leads to enhanced reaction kinetics.[8,9] More interestingly, unique conditions open new reaction pathways and produce mechano-exclusive products, expanding the boundaries of chemical synthesis.[10]

With its rapid advance, mechanochemists have tried to understand the exact events inside mechanochemistry.[11−14] In the case of ball milling, the hot spot theory had prevailed, which explained that impact causes an extreme level of localized temperature and pressure and promotes chemical transformations of solid chemicals.[15−17] However, recent studies have proposed different ideas. In the case of soft matter, mechanochemical reactions can be understood based on similarities with solution reactions. Many examples exhibit solution-like kinetics and mechanisms as well as dependence on bulk temperature.[18−22] However, the mechanical force-induced molecular dynamics sometimes differ from the solution's,[16,23−25] which leads to mechano-exclusive transformations.[10,26,27]

In solution reactions, we dissolve all reagents so that all molecules are evenly dispersed and ready to react. Solid-state ball milling is different. Heterogeneous starting mixtures undergo chemical transformation by mechanical force, some-

Received: March 21, 2025
Revised: May 21, 2025
Accepted: May 22, 2025
Published: May 29, 2025

times faster than in solution. Interestingly, mechanochemical conditions are able to accommodate reactant combinations that are unfavorable in solution, such as orthogonally soluble reagents. Thus, the study of how mechanochemical reactions proceed is of great interest. Several reaction models have been developed. James and co-workers proposed a pseudofluid model.[17] They tracked the reaction of ZnO and imidazole, producing zinc imidazolate frameworks (ZIF-6). The reaction rate was found to be responsive to the collision frequency, leading them to conclude that the reaction rate was dependent on the removal of product layers through attrition and mixing. This led them to conclude that reagents remain in a heterogeneous phase and the reaction occurs at the surface of particles.

However, mechanochemical cocrystallization presents a different view. In a binary system, two heterogeneous reagents undergo mixing and produce cocrystals in which two molecules are dispersed evenly into a homogeneous state. Sometimes, they reach the final structures quickly on a minute scale.[28−32] The simulation work by Ferguson describes the molecular movement during cocrystallization.[33] Mixing occurs readily, even during low-energy collisions through localized amorphizations. The movement of molecules during the contact of particles has also been studied. Recently, Halasz and co-workers directly observed fast atomic and molecular exchange between particles under ball milling conditions.[34] Our team also recently reported the copolymerization of hydrophilic and hydrophobic monomers.[35,36] Molecular level dispersion produced copolymers with one glass transition temperature, implying the molecular level distribution of two immiscible molecules. These observations collectively support the idea that mechanochemical reactions may proceed in a homogeneous phase.

The previously described studies have not addressed this question: Is a mechanochemical reaction homogeneous or heterogeneous? If the chemical transformation mostly occurs on the contact surface, then it is a heterogeneous reaction. When the solid-state molecular mixing is faster than the reaction, homogeneous mixtures of particles would form first, and a homogeneous reaction could be viable (Figure 1).

In this article, we conducted a model study that can trace its mixing status and produce distinctive products: a catalytic copolymerization of L-lactide (LLA) and D-lactide (DLA) (Figure 2). A nonstereoselective catalyst under homogeneous conditions would link LLA and DLA randomly, producing atactic polylactic acids (*a*-PLA), analogous to a solution reaction. However, we expect that the same catalyst under heterogeneous conditions would produce isotactic multiblock PLA. Upon initiation of the reaction, each reactive chain end enters one particle, which is one monomer domain, and grows into a homopolymer chain. Mechanical mixing could move the chain end to another monomer particle to afford the second domain and induce propagation of the second block. If each active chain end navigates among individual particles, then multiblock copolymers will form. Thus, structural analysis of the PLA products from mechanochemical ball milling would help us to understand the nature of the mechanochemical reactions.

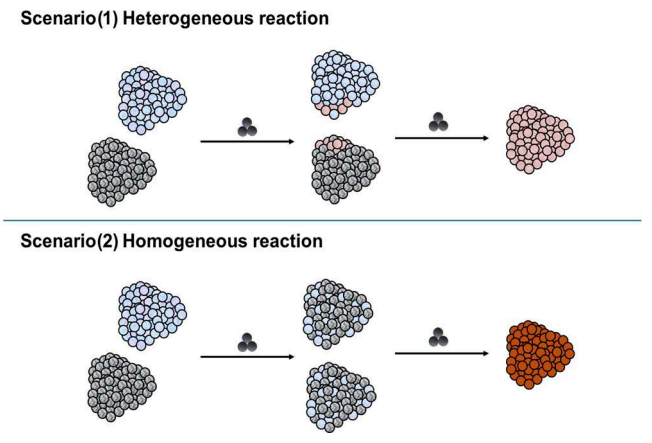

Figure 1. Mixing and reaction scenarios for solid-state mechanochemical reactions.

RESULTS AND DISCUSSION

To elucidate the mixing status, we collected powder X-ray diffraction (PXRD) data of the solid lactide mixture *in situ* and *ex situ*. An equal quantity mixture of LLA and DLA was placed in the ball-milling apparatus, and its phase change was monitored over different milling durations (Figure 3). Each lactide sample was premilled before mixing to skip a comminution step, ensuring that the mixing phenomenon becomes a major event.

In situ PXRD monitoring was conducted on an equimolar mixture of LLA and DLA (100 mg each). The mixture was added to a 13 mL poly(methyl methacrylate) jar with three stainless steel (SS) balls of 5 mm diameter. The phase change that occurred during vibratory milling (at 30 Hz in a InSolido IST636 mill) was monitored in real-time using synchrotron PXRD at the Deutsches Elektronen-Synchrotron (λ = 0.207365 Å) (Figure 3A). The initial signals from chiral LLA and DLA disappeared quickly, within 5 min. A new set of peaks appeared immediately, indicative of an instantaneous structural change induced by mechanical force.

The parallel *ex situ* PXRD resolved the identity of the new peaks (Cu Kα source, λ = 1.54 Å). The same mixture was added to a 10 mL SS jar containing three 5 mm diameter SS balls (Figure 3B). After each specified vibratory milling interval (at 30 Hz in a Retsch MM400 mill), the mixture was analyzed by PXRD to obtain mixing information. Similar to the *in situ* observation, the initial phase of the chiral compounds quickly diminished, within a minute. The resulting PXRD pattern was compared to that from a racemic LLA and DLA crystal phase, which was prepared in a separate process (dissolving a 1:1 mixture of LLA and DLA in dichloromethane, then removing the solvent).[37] The PXRD pattern from the racemic mixture was identical with that from milling. This led us to conclude that the solid-state mixture of LLA and DLA quickly reached a nearly complete homogeneous state under mechanochemical ball milling conditions. In addition, no transient peaks belonging to other phases were observed. A similar observation was recently reported by Bolm and Wiegand using solid-state NMR spectroscopy.[38] A mixture of (*S*) and (*R*)-α-(trifluoromethyl)lactic acid reached a racemic state within 30 s milling (25 Hz, 7 mm ball in 1.5 mL jar). This suggests that a mechanochemical mixture could lose its heterogeneous character within the initial stage of milling, as it is rapidly homogenized.

Subsequently, we examined the effect of milling parameters on phase change through *ex situ* PXRD analysis (Figure 4). We began by evaluating the influence of different ball and jar materials and ball sizes, which directly modulate the impact

https://doi.org/10.1021/jacsau.5c00322
JACS Au 2025, 5, 2720−2727

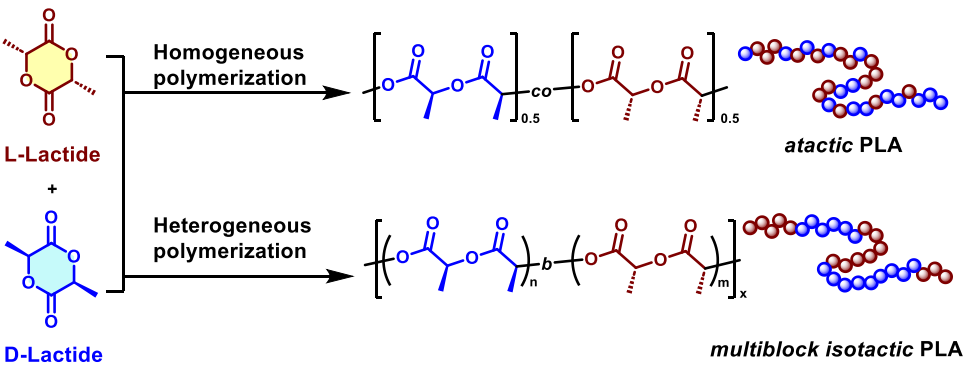

Figure 2. Distinctive products obtained from the homo- or heterogeneous copolymerization of LLA and DLA.

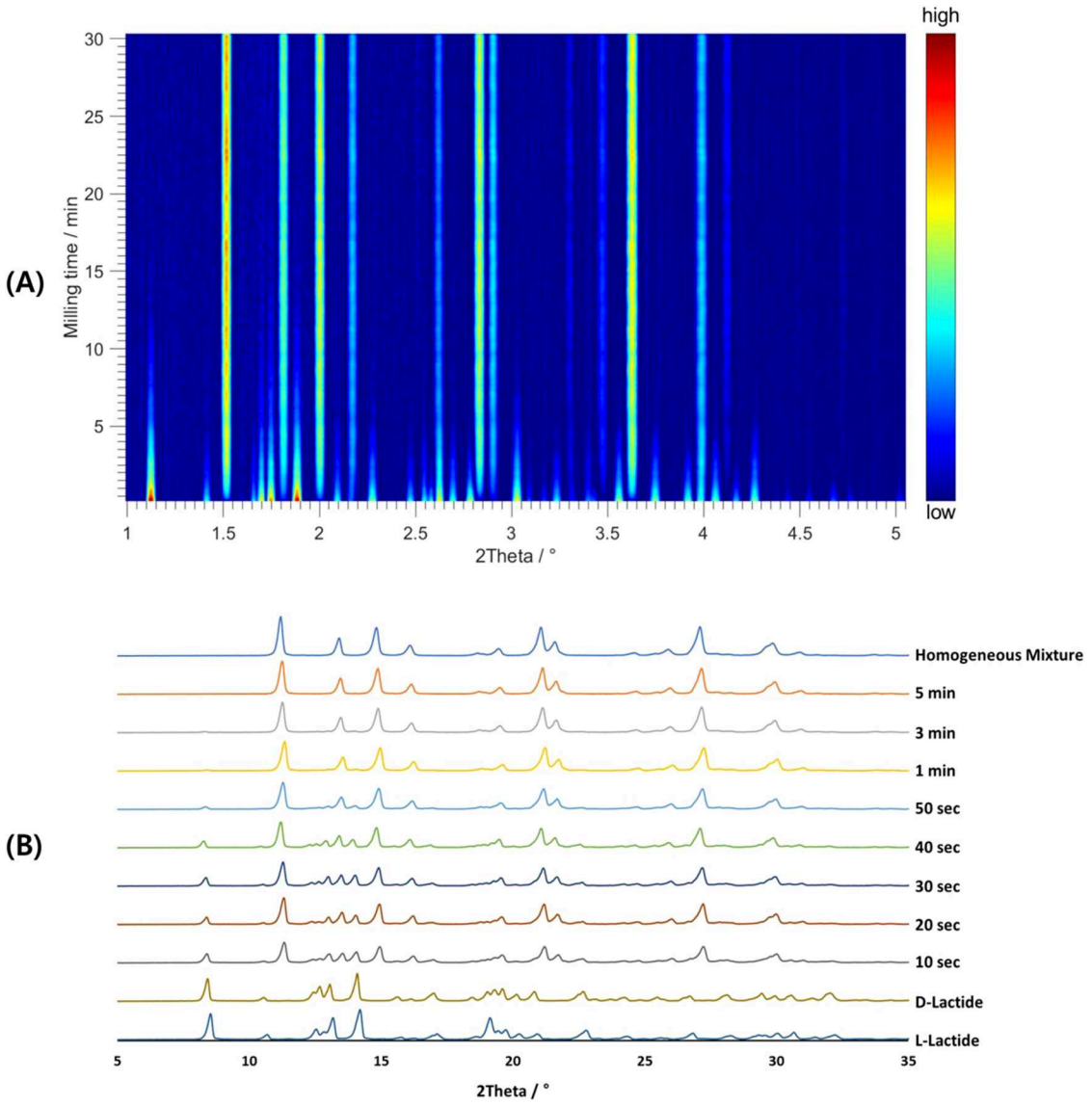

Figure 3. (A) *In situ* monitoring of ball milling of an equimolar mixture of DLA and LLA by synchrotron PXRD (λ = 0.207365 Å) using three 5 mm SS balls in a 13 mL PMMA jar at 30 Hz. The intensity color code is given on the right. (B) *Ex situ* monitoring of PXRD (λ = 1.54 Å) patterns of an equimolar mixture of LLA and DLA subjected to ball milling using three 5 mm SS balls in a 10 mL SS jar at 30 Hz. The homogeneous mixture was produced with a solution process for comparison.

force.[39] Notably, 30 Hz milling with SS balls (5 mm, 3 balls) in a 10 mL SS jar significantly accelerated homogenization compared to zirconia (Zr) balls and jar (with otherwise the same conditions) (Figure 4A). With the Zr ball, a substantial amount of the chiral lactide phase remained even after 5 min, whereas the denser SS balls achieved a fully racemic state within 1 min. Similarly, employing larger Zr balls (8 mm) under both one-ball (Figure 4B left) and three-ball milling

https://doi.org/10.1021/jacsau.5c00322
JACS Au 2025, 5, 2720−2727

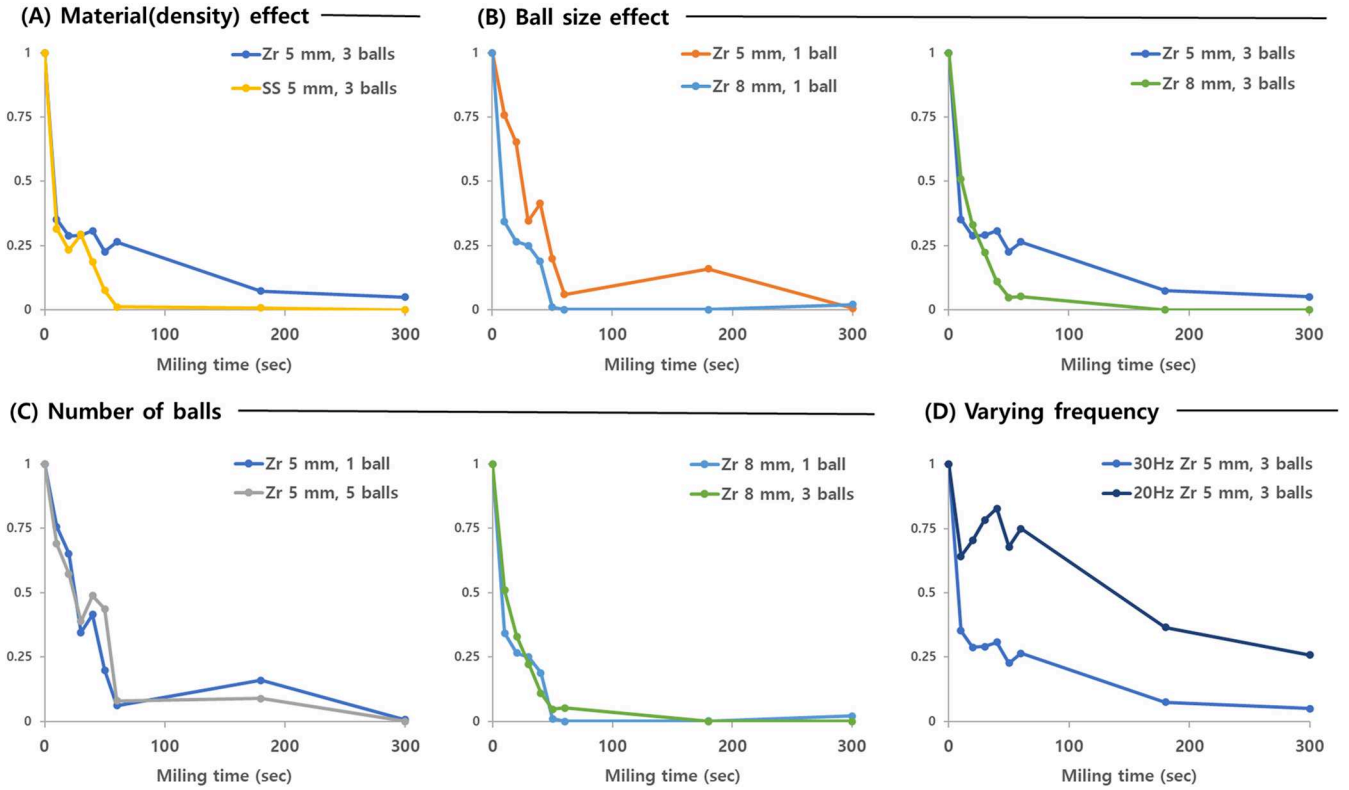

Figure 4. Influence of milling parameters on the phase change of the LLA and DLA mixtures. Vertical axes correspond to the area of 14° peaks from PXRD, normalized to the initial LLA intensity. All experiments were conducted in a 10 mL Zr jar except (A) SS 5 mm with 3 balls, which used a 10 mL SS jar. A vibration frequency of 30 Hz was applied except (D) 20 Hz Zr 5 mm with 3 balls.

Table 1. Mechanochemical Solid-State Ball-Milling Copolymerization of LLA and DLA

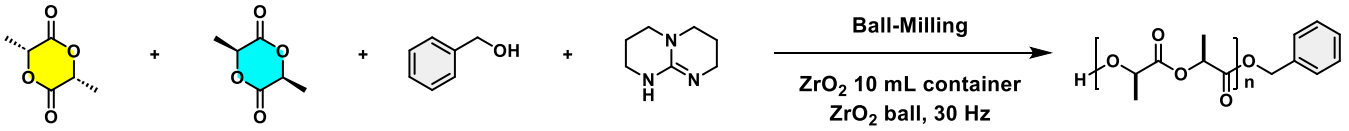

L-Lactide 100 mg (0.5 eq.) + **D-Lactide** 100 mg (0.5 eq.) + **BnOH** 1.5 uL (0.01 eq.) + **TBD** 1.0 mg (0.005 eq.)

E_n	balls	time (min)	M_n (kg/mol)[a]	M_w (kg/mol)[a]	$Đ$[a]	conv. (%)[b]	P_m[c]
1	Zr 8 mm × 3 mm	1	5.7	9.4	1.65	12	0.82
2	Zr 8 mm × 3 mm	10	14.9	25.5	1.70	99	0.61
3	Zr 5 mm × 5 mm	10	5.4	8.4	1.56	23	0.67
4[d]	SS 8 mm × 3 mm	1	8.3	13.6	1.63	27	0.72
5	Zr 8 mm × 3 mm toluene 20 μL	1	13.3	22.8	1.71	49	0.78

[a]Determined by GPC calibrated with polystyrene standards in tetrahydrofuran at 40 °C. [b]Determined by ^{1}H NMR spectroscopy. [c]Determined by ^{1}H homodecoupled NMR spectroscopy. [d]SS 10 mL container was used.

(Figure 4B right) conditions facilitated faster mixing than did 5 mm balls, indicating that the magnitude of impact force plays a direct role in material homogenization. We next investigated the influence of the ball quantity, hypothesizing that increasing the number of balls might enhance the collision frequency and improve mixing (Figure 4C). Two sets of data were collected: one using 5 mm balls in quantities of one and five, and another using 8 mm balls in quantities of one and three. In both cases, varying the number of balls did not significantly affect the mixing efficiency. Lastly, we explored the effect of the vibration frequency (Figure 4D). Lower frequencies, such as 20 Hz, significantly slowed the mixing process, leaving a substantial amount of the chiral lactide phase even after 5 min of milling. Low frequency leads to slow movement of balls and jar, causing low impact energy and collision frequencies. Thus, low frequency yields poor mixing. Overall these observations collectively underscore that the magnitude of impact plays a more critical role in promoting phase change than collision frequency.

Next, the copolymerization and structural changes upon phase change of LLA and DLA were investigated. Given the rapid phase change to a homogeneous state, we aimed to identify a copolymerization system capable of reaching a significant polymerization rate within the time frame. Addi-

https://doi.org/10.1021/jacsau.5c00322
JACS Au 2025, 5, 2720−2727

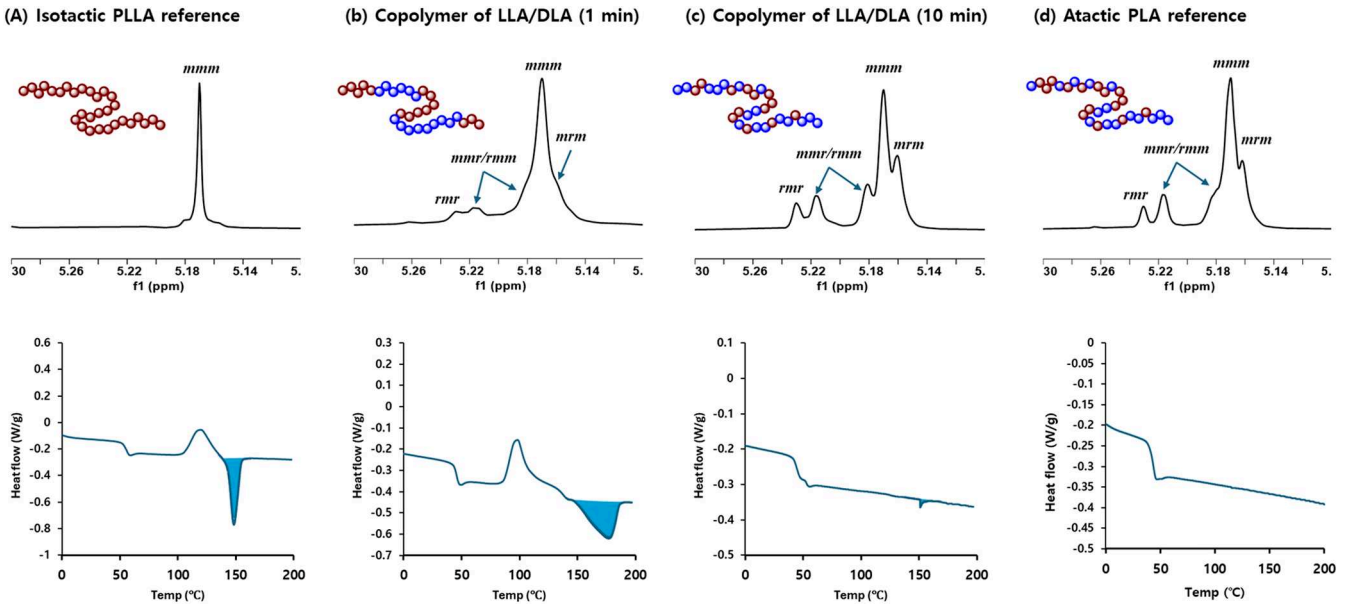

Figure 5. ^{1}H homodecoupled NMR (top, methine region) and DSC spectra (bottom) of (a) isotactic PLLA, (b) copolymer from LLA and DLA after 1 min of ball milling, (c) copolymer from LLA and DLA after 10 min of ball milling, and (d) *a*-PLA from solution synthesis.

tionally, it was critical for the catalyst to exhibit low stereoselectivity, ensuring that the polymer composition would reflect the mixing conditions. Leveraging our previous research on mechanochemical lactide polymerization, we selected 1,5,7-triazabicyclo[4.4.0]dec-5-ene (TBD) as the catalyst. Known for its high polymerization rate in both solution and solid-state ball milling, TBD also demonstrates low stereoselectivity toward racemic LA.[40−42]

The copolymerization was conducted under the conditions outlined in Table 1. An equimolar amount of LLA and DLA (100 mg each) was combined in a 10 mL Zr jar with 1 mol % benzyl alcohol as initiator and 0.5 mol % TBD catalyst. The mixture was subjected to ball milling at 30 Hz with the given numbers and size of Zr balls in an MM400 mill for the indicated duration. After milling, the solid product was dissolved and quenched in chloroform with acetic acid. The isolated polymer products were analyzed for tacticity by ^{1}H homodecoupled NMR (Figure 5, top),[43] thermal properties via differential scanning calorimetry (DSC) (Figure 5, bottom), and molecular weights through gel permeation chromatography (GPC).

The one min polymerization with three 8 mm Zr balls at 30 Hz yielded PLA with a conversion of 12%, a number-average molecular weight (M_n) of 5.7 kg/mol, and a molecular weight dispersity ($Đ$) of 1.65 (Table 1, entry 1). Comparisons of the ^{1}H homodecoupled NMR methine region with reference isotactic PLLA confirmed its isotactic preference during polymerization (Figure 5A,B). The isotactic PLLA derived from pure LLA exclusively exhibited meso (*m*) dyads, with the signal at 5.17 ppm corresponding to the methine signal of the *mmm* tetrad, as observed in the ^{1}H homodecoupled NMR spectrum (Figure 5A, top). In contrast, the copolymerization of LLA and DLA would introduce racemic dyad (*r*) tetrads at each junction between DLA and LLA. Consequently, the ^{1}H homodecoupled NMR spectrum would exhibit peaks corresponding to *mmr* (5.18 and 5.22 ppm), *rmm* (5.18 and 5.22 ppm), *mrm* (5.16 ppm), and *rmr* (5.23 ppm) tetrads in addition to *mmm*. The polymer obtained from one min solid-state ball milling predominantly displayed the primary isotactic *mmm* tetrad peak at 5.17 ppm, along with minor peaks corresponding to racemic connections (Figure 5B, top). The probability of meso enchainment (P_m) was 0.82,[14] indicative of isotactic PLA, suggesting that LLA-to-LLA and DLA-to-DLA propagations were predominant. This implies that polymerization primarily proceeded under heterogeneous conditions. DSC analysis further confirmed the presence of a block structure. The regulated side-chain architecture promotes efficient intermolecular interactions, leading to crystallinity. Both the PLA obtained from one min ball milling and the reference PLLA exhibited clear endothermic melting transitions above 130 °C (blue areas in Figure5A,B, bottom), consistent with isotactic structures. Notably, the melting peak of the polymer derived from the racemic mixture appeared at a higher temperature than that of the reference PLLA, which is attributed to stereocomplexation between PLLA and PDLA blocks—known to exhibit stronger intermolecular interactions than PLLA alone.[44,45]

With an extended reaction time of 10 min, monomer conversion reached 99%, while P_m decreased to 0.61 (Table 1, entry 2). In the ^{1}H homodecoupled NMR spectrum, tetrads containing racemic dyads became significantly more prominent compared to the product obtained after 1 min of polymerization (Figure 5C, top). After accounting for the isotactic fraction observed at the 1 min mark, the stereoselectivity from 1 to 10 min was calculated as P_m = 0.58, indicating a largely nonselective distribution. The overall tetrad distribution closely resembled that of PLA obtained under homogeneous solution conditions by using a TBD catalyst (Figure 5D, top). The final polymer underwent a brief period under heterogeneous conditions, followed predominantly by homogeneous conditions. As a result, the polymer is expected to contain short isotactic segments within a largely atactic structure. This structural feature is clearly reflected in the DSC analysis, which shows a significantly diminished melting signal around 150 °C (Figure 5C, bottom)—a feature absent in the DSC trace obtained under purely homogeneous solution conditions (Figure 5D, bottom).

https://doi.org/10.1021/jacsau.5c00322
JACS Au 2025, 5, 2720−2727

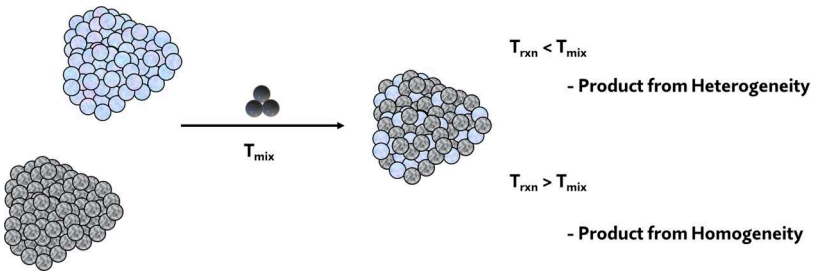

Figure 6. Mixing and reaction rate consideration for a solid-state mechanochemical reaction environment.

Polymerizations under both weaker and stronger mechanochemical conditions were investigated (Table 1, entries 3 and 4). The use of smaller balls, which was expected to prolong the heterogeneous phase, significantly slowed the polymerization rate, yielding only 23% conversion after 10 min of milling. ^{1}H NMR analysis revealed a P_m value of 0.67, suggesting that the reaction predominantly proceeded under homogeneous conditions. In contrast, the use of heavier balls—three 8 mm SS balls in a 10 mL SS jar, increased the conversion to 27% within one min, compared to 12% with three 8 mm zirconia (Zr) balls (entry 3 *vs* entry 1). Simultaneously, the stronger mechanical impact enhanced mixing, resulting in a relatively lower P_m value (0.72). However, the corresponding DSC trace (Figure S26) exhibited a distinct melting peak, indicating the formation of isotactic blocks capable of crystallization at an early stage.

Further investigation was carried out to examine the effect of liquid-assisted grinding (LAG) (Table 1, entry 5). LAG, which involves the addition of a small amount of liquid to a ball-milling reaction, is a well-established method for accelerating or even enabling mechanochemical transformations.[2] In our previous study on polylactide synthesis, toluene was shown to enhance the reaction rate while suppressing chain degradation.[41] In the present work, we evaluated its influence on mixing by adding a small amount of toluene (20 μL) to 200 mg of the lactide mixture. Ball milling for one min with three 8 mm Zr balls significantly increased the conversion to 49% and yielded a high-molecular-weight polymer, while the P_m value only slightly decreased to 0.78. The DSC trace (Figure S30) exhibited a high melting temperature near 170 °C, indicating a more ordered microstructure. In this case, LAG selectively enhanced the reactivity without significantly affecting the mixing state. Further studies are currently underway to explore the effects of varying the LAG conditions on mixing behavior.

CONCLUSIONS

The investigation into phase transition monitoring and polymerization product properties of racemic lactide mixtures under solid-state ball milling conditions revealed a facile shift from heterogeneous to homogeneous conditions. The reaction outcome was dictated by the phase: isotactic PLA formed in the early stage under heterogeneous solid-state conditions, while atactic PLA was obtained after the transition to a homogeneous mixture. This behavior represents a unique feature of mechanochemistry. In terms of molecular-level explanation, previous studies have primarily explained mechanochemical solid-state reactions based on heterogeneous surface conditions. However, the rapid phase transformation observed in this study suggests that mechanochemical reactions can also proceed under homogeneous conditions.

When a mechanochemical reaction undergoes a transition, it is essential to consider both the mixing time (T_{mix}) and the reaction time (T_{rxn}) in the process design (Figure 6). If T_{mix} is slower than T_{rxn}, then the reaction is predominantly governed by heterogeneity. Conversely, if T_{mix} is faster than T_{rxn}, then the system tends to exhibit selectivity similar to that of homogeneous solution conditions.

Although this study presents a single example, it does not aim to represent all of the mechanochemical systems. Rather, it proposes the hypothesis that homogeneous phases can exist and play a critical role in certain mechanochemical reactions. This perspective adds a new dimension to the interpretation of both past and future mechanochemical studies. We are currently reevaluating previous examples of mechanochemical reactions with the new possibility of homogeneity in mind.

MATERIALS AND METHODS

D- and L-lactides were sourced from Natureworks. Each batch was purified through recrystallization four times in ethyl acetate. Each chiral lactide (3 g) was premilled before mixing and polymerization, using three Zr 8 mm balls in a 10 mL Zr container. The ball milling was conducted for 10 min at 30 Hz in a Retsch MM400 mill. Other reagents and solvents were purchased from commercial sources (Aldrich, Alfa Aesar, TCI, or Acros, and Daejeong Chemical) and were used without further purification.

MEASUREMENT

In situ monitoring of ball milling reactions by synchrotron powder X-ray diffraction (PXRD) was performed at the P02.1 beamline at PETRA III, DESY (Hamburg, Germany). We used jars made of poly(methyl)methacrylate (PMMA, 13 mL internal volume). Ball milling was conducted with the IST-636 mixer mill (InSolido Technologies, Croatia, Zagreb) operating at 30 Hz. The X-ray beam (λ = 0.207365 Å) was set to pass through the bottom of the PMMA reaction vessel. Exposure time was set to 10 s. Diffraction data were collected on a PerkinElmer XRD1621 flat-panel detector positioned 1595 mm from the sample, which consisted of an amorphous Si sensor equipped with a CsI scintillator (pixel number: 2048 × 2048, pixel size: 200 × 200 μm^2). To obtain the classic one-dimensional PXRD pattern, the two-dimensional diffraction images were integrated with the in house developed Python script. Two-dimensional (2D) time-resolved plots of *in situ* monitoring data were created in MATLAB and the background of each diffraction pattern was subtracted prior to plotting using the Sonneveld-Visser algorithm.[46] *Ex situ* PXRD analysis was carried out using a Rigaku Miniflex instrument with a Cu Kα source (λ = 1.54 Å) at an accelerating voltage of 40 kV and emission current of 15 mA. The diffraction patterns were recorded using the step scan mode with a step size of 0.02° and a counting time of 1 s for each step.

https://doi.org/10.1021/jacsau.5c00322
JACS Au 2025, 5, 2720−2727

■ ASSOCIATED CONTENT

Supporting Information

The Supporting Information is available free of charge at https://pubs.acs.org/doi/10.1021/jacsau.5c00322.

PXRD, NMR, and DSC data (PDF)

■ AUTHOR INFORMATION

Corresponding Authors

Kyoungsoo Kim − *Department of Chemistry, Jeonbuk National University, Jeonju 54896, Republic of Korea; Research Institute of Physics and Chemistry, Jeonbuk National University, Jeonju 54896, Republic of Korea;* orcid.org/0000-0002-2042-0913; Email: kyoungsookim@jbnu.ac.kr

Jeung Gon Kim − *Department of Chemistry, Jeonbuk National University, Jeonju 54896, Republic of Korea; Research Institute of Materials and Energy Sciences & Department of JBNU-KIST Industry-Academia Convergence Research, Jeonbuk National University, Jeonju 54896, Republic of Korea;* orcid.org/0000-0003-1685-2833; Email: jeunggonkim@jbnu.ac.kr

Authors

Eun Sul Go − *Department of Chemistry, Jeonbuk National University, Jeonju 54896, Republic of Korea*

Eun Ji Hong − *Department of Chemistry, Jeonbuk National University, Jeonju 54896, Republic of Korea*

Ji Yeong Lee − *Department of Chemistry, Jeonbuk National University, Jeonju 54896, Republic of Korea*

Tomislav Stolar − *BAM Federal Institute for Materials Research and Testing, 12489 Berlin, Germany;* orcid.org/0000-0002-9824-4462

Gregory I. Peterson − *Department of Chemistry and Research Institute of Basic Science, Incheon National University, Incheon 22012, Republic of Korea;* orcid.org/0000-0002-5944-4381

Franziska L. Emmerling − *BAM Federal Institute for Materials Research and Testing, 12489 Berlin, Germany*

Complete contact information is available at: https://pubs.acs.org/10.1021/jacsau.5c00322

Author Contributions

The manuscript was written through contributions of all authors. CRediT: E.S.G., E.J.H. Investigation, Formal Analysis, Data Curation of *ex situ* PXRD and polymerization study; J.Y.L. Investigation and Validation of polymerization study; T.S. Investigation, Formal Analysis, Data Curation of *in situ* PXRD; G.I.P Conceptualization, Project administration; F.L.E. Supervision,Project Administration on *in situ* PXRD; **K.K. Conceptualization, Methodology, Supervision on PXRD study; J.G.K. Conceptualization, Supervision, Project administration, Funding acquisition.**

Notes

The authors declare no competing financial interest.

■ ACKNOWLEDGMENTS

This research was supported by the National Research Foundation of Korea (RS2024-00342198, RS2024-00443714) and the Samsung Science & Technology Foundation (SRFC-MA1902-05) to J.G.K. T.S. acknowledges DESY (Hamburg, Germany) for the provision of experimental facilities. Parts of this research were carried out at PETRA III, beamline P02.1. Beamtime was allocated for proposal I-20231186.

■ REFERENCES

(1) James, S. L.; Friščić, T. Mechanochemistry. *Chem. Soc. Rev.* **2013**, *42*, 7494−7496.

(2) Do, J.-L.; Friščić, T. Mechanochemistry: A Force of Synthesis. *ACS Cent. Sci.* **2017**, *3*, 13−19.

(3) Andersen, J.; Mack, J. Mechanochemistry and Organic Synthesis: From Mystical to Practical. *Green Chem.* **2018**, *20*, 1435−1443.

(4) Krusenbaum, A.; Grätz, S.; Tigineh, G. T.; Borchardt, L.; Kim, J. G. The Mechanochemical Synthesis of Polymers. *Chem. Soc. Rev.* **2022**, *51*, 2873−2905.

(5) Rizzo, A.; Peterson, G. I. Progress toward Sustainable Polymer Technologies with Ball-Mill Grinding. *Prog. Polym. Sci.* **2024**, *159*, No. 101900.

(6) Fantozzi, N.; Volle, J.-N.; Porcheddu, A.; Virieux, D.; García, F.; Colacino, E. Green Metrics in Mechanochemistry. *Chem. Soc. Rev.* **2023**, *52*, 6680−6714.

(7) Alić, J.; Schlegel, M.-C.; Emmerling, F.; Stolar, T. Meeting the UN Sustainable Development Goals with Mechanochemistry. *Angew. Chem., Int. Ed.* **2024**, *63*, No. e202414745.

(8) Howard, J. L.; Cao, Q.; Browne, D. L. Mechanochemistry as an Emerging Tool for Molecular Synthesis: What Can It Offer? *Chem. Sci.* **2018**, *9*, 3080−3094.

(9) Park, S.; Kim, J. G. Mechanochemical Synthesis of Poly-(Trimethylene Carbonate)s: An Example of Rate Acceleration. *Beilstein J. Org. Chem.* **2019**, *15*, 963−970.

(10) Hernández, J. G.; Bolm, C. Altering Product Selectivity by Mechanochemistry. *J. Org. Chem.* **2017**, *82*, 4007−4019.

(11) Friščić, T.; Halasz, I.; Beldon, P.; Belenguer, A. M.; Adams, F.; Kimber, S. A. J.; Honkimäki, V.; Dinnebier, R. E. Real-Time and In Situ Monitoring of Mechanochemical Milling Reactions. *Nat. Chem.* **2013**, *5*, 66−73.

(12) Michalchuk, A. A. L.; Emmerling, F. Time-Resolved In Situ Monitoring of Mechanochemical Reactions. *Angew. Chem., Int. Ed.* **2022**, *61*, No. e202117270.

(13) Užarević, K.; Halasz, I.; Friščić, T. Real-Time and In Situ Monitoring of Mechanochemical Reactions: A New Playground for All Chemists. *J. Phys. Chem. A* **2015**, *6*, 4129−4140.

(14) Lukin, S.; Užarević, K.; Halasz, I. Raman spectroscopy for real-time and in situ monitoring of mechanochemical milling reactions. *Nat. Protoc.* **2021**, *16*, 3492−3521.

(15) Tricker, A. W.; Samaras, G.; Hebisch, K. L.; Realff, M. J.; Sievers, C. Hot Spot Generation, Reactivity, and Decay in Mechanochemical Reactors. *Chem. Eng. J.* **2020**, *382*, No. 122954.

(16) Zholdassov, Y. S.; Kwok, R. W.; Shlain, M. A.; Patel, M.; Marianski, M.; Braunschweig, A. B. Kinetics of Primary Mechano-chemical Covalent-Bond-Forming Reactions. *RSC Mechanochem.* **2024**, *1*, 11−32.

(17) Bowden, F. P.; Yoffe, A. D.; Hudson, G. E. Initiation and Growth of Explosion in Liquids and Solids. *Am. J. Phys.* **1952**, *20* (4), 250−251.

(18) Ma, X.; Yuan, W.; Bell, S. E. J.; James, S. L. Better Understanding of Mechanochemical Reactions: Raman Monitoring Reveals Surprisingly Simple 'Pseudo-Fluid' Model for a Ball Milling Reaction. *Chem. Commun.* **2014**, *50*, 1585−1587.

(19) Andersen, J.; Mack, J. Insights into Mechanochemical Reactions at Targetable and Stable, Sub-Ambient Temperatures. *Angew. Chem., Int. Ed.* **2018**, *57*, 13062−13065.

(20) Andersen, J. M.; Mack, J. Decoupling the Arrhenius Equation via Mechanochemistry. *Chem. Sci.* **2017**, *8*, 5447−5453.

(21) Seo, T.; Toyoshima, N.; Kubota, K.; Ito, H. Tackling Solubility Issues in Organic Synthesis: Solid-State Cross-Coupling of Insoluble Aryl Halides. *J. Am. Chem. Soc.* **2021**, *143*, 6165−6175.

(22) Hutchings, B. P.; Crawford, D. E.; Gao, L.; Hu, P.; James, S. L. Feedback Kinetics in Mechanochemistry: The Importance of Cohesive States. *Angew. Chem., Int. Ed.* **2017**, *56*, 15252−15256.
(23) Zholdassov, Y. S.; Yuan, L.; Garcia, S. R.; Kwok, R. W.; Boscoboinik, A.; Valles, D. J.; Marianski, M.; Martini, A.; Carpick, R. W.; Braunschweig, A. B. Acceleration of Diels-Alder Reactions by Mechanical Distortion. *Science* **2023**, *380*, 1053−1058.
(24) Schüth, F.; Rinaldi, R.; Meine, N.; Käldström, M.; Hilgert, J.; Rechulski, M. D. K. Mechanochemical Depolymerization of Cellulose and Raw Biomass and Downstream Processing of the Products. *Catal. Today* **2024**, *234*, 24−30.
(25) Kobayashi, H.; Suzuki, Y.; Sagawa, T.; Kuroki, K.; Hasegawa, J.; Fukuoka, A. Impact of Tensile and Compressive Forces on the Hydrolysis of Cellulose and Chitin. *Phys. Chem. Chem. Phys.* **2021**, *23*, 15908−15916.
(26) Cuccu, F.; De Luca, L.; Delogu, F.; Colacino, E.; Solin, N.; Mocci, R.; Porcheddu, A. Mechanochemistry: New Tools to Navigate the Uncharted Territory of "Impossible" Reactions. *ChemSusChem* **2022**, *15*, No. e202200362.
(27) Ardila-Fierro, K. J.; Hernández, J. G. Intermediates in Mechanochemical Reactions. *Angew. Chem., Int. Ed.* **2024**, *63*, No. e202317638.
(28) Xiao, Y.; Wu, C.; Hu, X.; Chen, K.; Qi, L.; Cui, P.; Zhou, L.; Yin, Q. Mechanochemical Synthesis of Cocrystals: From Mechanism to Application. *Cryst. Growth Des.* **2023**, *23*, 4680−4700.
(29) Stolar, T.; Lukin, S.; Tireli, M.; Sović, I.; Karadeniz, B.; Kereković, I.; Matijašić, G.; Gretić, M.; Katančić, Z.; Dejanović, I.; di Michiel, M.; Halasz, I.; Užarević, K. Control of Pharmaceutical Cocrystal Polymorphism on Various Scales by Mechanochemistry: Transfer from the Laboratory Batch to the Large-Scale Extrusion Processing. *ACS Sustainable Chem. Eng.* **2019**, *7*, 7102−7110.
(30) Casali, L.; Carta, M.; Michalchuk, A. A. L.; Delogu, F.; Emmerling, F. Kinetics of the Mechanically Induced Ibuprofen−Nicotinamide Co-Crystal Formation by In Situ X-ray Diffraction. *Chem. Phys. Chem. Phys.* **2024**, *26*, 22041−22048.
(31) Teoh, T.; Ayoub, G.; Huskić, I.; Titi, H. M.; Nickels, C. W.; Herrmann, B.; Friščić, T. SpeedMixing: Rapid Tribochemical Synthesis and Discovery of Pharmaceutical Cocrystals without Milling or Grinding Media**. *Angew. Chem., Int. Ed.* **2022**, *61*, No. e202206293.
(32) Halasz, I.; Puškarić, A.; Kimber, S. A. J.; Beldon, P. J.; Belenguer, A. M.; Adams, F.; Honkimäki, V.; Dinnebier, R. E.; Patel, B.; Jones, W.; Štrukil, V.; Friščić, T. Real-Time In Situ Powder X-ray Diffraction Monitoring of Mechanochemical Synthesis of Pharmaceutical Cocrystals. *Angew. Chem., Int. Ed.* **2013**, *52*, 11538−11541.
(33) Ferguson, M.; Moyano, M. S.; Tribello, G. A.; Crawford, D. E.; Bringa, E. M.; James, S. L.; Kohanoff, J.; Del Pópolo, M. G. Insights into Mechanochemical Reactions at the Molecular Level: Simulated Indentations of Aspirin and Meloxicam Crystals. *Chem. Sci.* **2019**, *10*, 2924−2929.
(34) Lukin, S.; Tireli, M.; Stolar, T.; Barisic, D.; Blanco, M. V.; di Michiel, M.; Uzarevic, K.; Halasz, I. Isotope Labeling Reveals Fast Atomic and Molecular Exchange in Mechanochemical Milling Reactions. *J. Am. Chem. Soc.* **2019**, *141*, 1212−1216.
(35) Lee, G. S.; Lee, H. S.; Kim, N.; Shin, H. G.; Hwang, Y. H.; Lee, S. J.; Kim, J. G. Mechanochemical Synthesis of Ionic Polymers: Solid-State Ball-Milling Polymerization for Unrestricted Solubility Enabling Copolymerization of Immiscible Monomers. *Macromolecules* **2024**, *57*, 9408−9418.
(36) Lee, G. S.; Lee, H. W.; Lee, H. S.; Do, T.; Do, J.-L.; Lim, J.; Peterson, G. I.; Friščić, T.; Kim, J. G. Mechanochemical Ring-Opening Metathesis Polymerization: Development, Scope, and Mechano-Exclusive Polymer Synthesis. *Chem. Sci.* **2022**, *13*, 11496−11505.
(37) van Hummel, G. J.; Harkema, S.; Kohn, F. E.; et al. Structure of 3,6-Dimethyl-1,4-Dioxane-2,5-Dione [D-,D-(L-,L-)Lactide]. *Acta Crystallogr., Sect. B Struct. Crystallogr. Cryst. Chem.* **1982**, *38*, 1679−1681.
(38) Quaranta, C.; Silva, I. d'A. A.; Moos, S.; Bartalucci, E.; Hendrickx, L.; Fahl, B. M. D.; Pasqualini, C.; Puccetti, F.; Zobel, M.; Bolm, C.; Wiegand, T. Molecular Recognition in Mechanochemistry: Insights from Solid-State NMR Spectroscopy. *Angew. Chem., Int. Ed.* **2024**, *63*, No. e202410801.
(39) Jafter, O. F.; Lee, S.; Park, J.; Cabanetos, C.; Lungerich, D. Navigating Ball Mill Specifications for Theory-to-Practice Reproducibility in Mechanochemistry. *Angew. Chem., Int. Ed.* **2024**, *63*, No. e202409731.
(40) Lohmeijer, B. G. G.; Pratt, R. C.; Leibfarth, F.; Logan, J. W.; Long, D. A.; Dove, A. P.; Nederberg, F.; Choi, J.; Wade, C.; Waymouth, R. M.; Hedrick, J. L. Guanidine and Amidine Organocatalysts for Ring-Opening Polymerization of Cyclic Esters. *Macromolecules* **2006**, *39*, 8574−8583.
(41) Ohn, N.; Shin, J.; Kim, S. S.; Kim, J. G. Mechanochemical Ring-Opening Polymerization of Lactide: Liquid-Assisted Grinding for the Green Synthesis of Poly(Lactic Acid) with High Molecular Weight. *ChemSusChem* **2017**, *10*, 3529−3533.
(42) Moins, S.; Hoyas, S.; Lemaur, V.; Orhan, B.; Chiaie, K. D.; Lazzaroni, R.; Taton, D.; Dove, A. P.; Coulembier, O. Stereoselective ROP of *rac*- and *meso*-Lactides Using Achiral TBD as Catalyst. *Catalysts* **2020**, *10*, No. 620.
(43) Münster, K.; Raeder, J.; Walter, M. D. Synthesis and Characterisation of an Enantiomerically Pure Scandium Pentadienyl Complex and Its Application in the Polymerisation of *rac*-Lactide. *Dalton Trans.* **2022**, *51*, 986−997.
(44) Tsuji, H. Poly Lactide) Stereocomplexes: Formation, Structure, Properties, Degradation, and Applications. *Macromol. Biosci.* **2005**, *5*, 569−597.
(45) Lamers, B. A. G.; van Genabeek, B.; Hennissen, J.; de Waal, B. F. M.; Palmans, A. R. A.; Meijer, E. W. Stereocomplexes of Discrete, Isotactic Lactic Acid Oligomers Conjugated with Oligodimethylsiloxanes. *Macromolecules* **2019**, *52*, 1200−1209.
(46) Sonneveld, E. J.; Visser, J. W. Automatic Collection of Powder Data from Photographs. *J. Appl. Crystallogr.* **1975**, *8*, 1−7.

https://doi.org/10.1021/jacsau.5c00322
JACS Au 2025, 5, 2720−2727